Spectral measurements of alpha-induced radioluminescence in various gases

Brett, Jaclyn
Koehler, Katrina Elizabeth
Bischak, Michael
Famiano, Michael
Jenkins, Jared
Klan, Levi
Niraula, Prashantamani
Pancella, Paul
Lakis, Rollin Evan

To be published in: Nuclear Instruments and Methods in Physics Research Section A: Accelerators, Spectrometers, Detectors and Associated Equipment

DOI to publisher's version: 10.1016/j.nima.2017.08.056

Permalink to record: http://permalink.lanl.gov/object/view?what=info:lanl-repo/lareport/LA-UR-17-23981

Spectral Measurements of Alpha-induced Radioluminescence in Various Gases

Jaclyn Brett[a], Katrina E. Koehler[a,b], Michael Bischak[a], Michael Famiano[a], Jared Jenkins[a], Levi Klankowski[a], Prashantamani Niraula[a], Paul Pancella[a], Rollin Lakis[b]

[a]*Department of Physics, Western Michigan University, Kalamazoo, MI 49008*
[b]*Nuclear Engineering and Nonproliferation, Los Alamos National Laboratory, Los Alamos, NM 87544*

Abstract

Radioluminescent emission in Ar, N_2, O_2, and dry air at P=1 atm was observed induced by 5 MeV α particles. The wavelength range with a single detector spanned 250–1100 nm, extending the range well into the UV and IR bands with a single detector. Measured spectral lines for alpha-induced luminescence were corrected for detector transmission and intensities compared to previous work. The exploration of multiple gases over a wide frequency range opens the door to security and remote sensing applications, where different environments are routinely encountered. This work provides spectra that can be used in guiding future filter development focusing on remote alpha detection.

Keywords: Radioluminescence, Air fluorescence, Imaging of alpha emitters, Optical detection of alpha emitters, Stand-off detection of alpha emitters

1. Introduction

Luminescence of gases occurs when charged particles transfer their kinetic energy to secondary electrons in a collision. These gas molecules are excited and, upon de-excitation, emit photons with energies corresponding to characteristic electron transitions. In air, the primary molecules excited are N_2 molecules [1]. Induced luminescence can be due to different types of ionizing radiation. For example, extensive air shower cosmic rays produce luminescence in air in the

300–430 nm range and experiments done with electron beams of similar energies have found nearly all of the luminescence was from de-excitations in N_2 [2, 3, 4].

Because alpha particles have a short range in gas, they are difficult to detect directly at ranges greater than $\sim$10 cm. However, photons from alpha-induced luminescence can be detected from a larger distance as the photon mean-free-path in gases at 1 atm is much larger. The alpha-induced luminescence photons have a range of wavelengths spanning the UV to the IR spectrum [5, 6, 7, 8]. It was found that the light intensity scales with total alpha energy loss in air, with 19 ± 3 photons per MeV for 45% humidity [7, 6].

A significant amount of work has been done with remote detection of alpha-induced luminescence [9, 5, 10, 11, 12, 13, 14, 15, 16, 17, 18, 19, 20, 6, 21, 22, 23, 7, 24]. Luminescence imaging was done with UV-sensitive film, charge-coupled device (CCD) cameras, intensified CCD cameras, electron-multiplying CCD cameras, and PMTs used as pixels. Many of these results consist of a superimposed image with the UV alpha-induced luminescent light taken in an otherwise dark environment on an image taken in normal lighting to show the range of luminescence from alpha particles and the possibility of detecting alpha particles remotely. Because of the difficulty involved in the production of images in dark environments for nuclear safety, security, and safeguards applications, developing an imaging system that can handle regular room-lighting conditions is desirable. This can be done by applying custom filters to maximize the radioluminescent light and minimize background light.

Further progress toward practical detection of alpha radiation in air requires detailed study of the induced light. Optical filtering has been used to suppress background light in order to improve the signal-to-background ratio, necessary in any useful detector system [22, 24]. Prior work has resulted in the spectra of emitted light from electrons losing energy in air [2, 3, 4], as well as published data on the wavelength dependence of alpha-induced radioluminescence in air [25, 26, 5, 16, 7] and specific gases like nitrogen and the noble gases [27, 28, 8, 29]. However, little quantitative data over a comprehensive range of wavelengths and gases exists because these spectra are published as images of photographic plates. Quantitative results can be found for air [5, 16, 7] and argon [28]. Some data [7] give quantitative results in the deep UV (below 300 nm) for air as well as a low resolution study of the alpha-luminescence spectrum in argon [28]. A careful measurement of alpha-induced luminescence in various gases can be used to optimize filter designs for various environments. In this work, the photon spectra from 5 MeV alpha particles in N_2, O_2, Ar, and air were studied.

2. Experimental Method

To measure the alpha-induced luminescent spectrum, a High Voltage Engineering Corporation 6-MV model EN tandem Van de Graaff accelerator at Western Michigan University was used to produce a 56 nA beam of 7.5 MeV alpha particles with a beam diameter of 4.7 mm. The beam intensity was 1.75×10^{11} alpha particles/second. The alpha-particles were incident on a 25 μm-thick 100HN Kapton Polyimide film window into a dark pressure chamber. Calculations using the Stopping and Range of Ions in Matter (SRIM) code showed the alpha particles to have an average of 5.0 MeV after passing through the window [30]. The chamber was filled with the different available gasses and kept constantly pressurized at 1 atm. Individual runs for a particular gas were done in which 5 MeV α-particles were incident in the chamber from the accelerator beam. Because this work presents a practical application for security purposes, for example, the remote sensing of alpha-emitting sources in gas hoods, 5 MeV α particles, roughly the energy of emitted alphas from fission chain decay, were chosen for the initial test. Switching between gases was done by evacuating the chamber completely, flushing fill lines with the new gas, evacuating the chamber again, and filling the chamber with gas.

For each gas, data were taken with the UV-optimized optical setup shown in Figure 1. The setup consisted of two parabolic mirrors. One mirror reflected the light emitted from the gas into a second mirror, which focused the light into an optical fiber[1]. All of these components were housed within the chamber, so

[1]The setup included a MPD129-F01 mirror, RC12SMA-F01 collimator, M92L02 200 μm

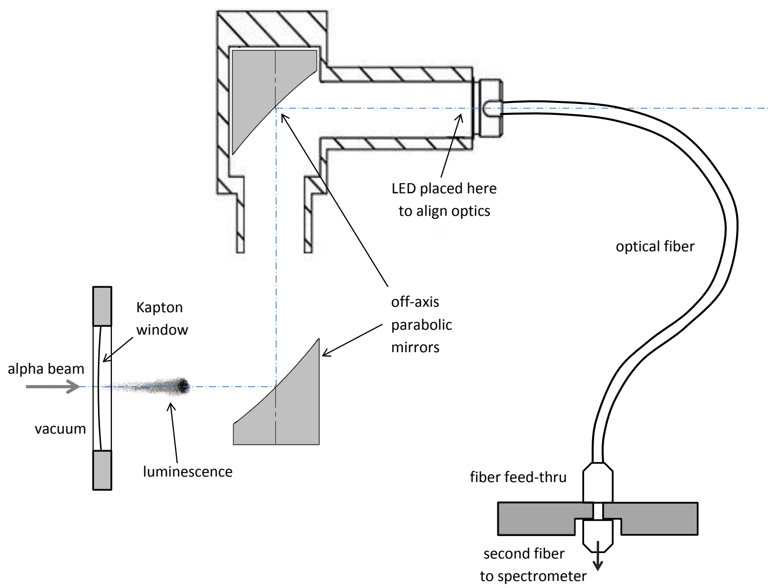

Figure 1: Diagram of the optical setup used for this experiment showing the parabolic mirrors, optical fibers, chamber feedthrough, and spectrometer (Not to scale).

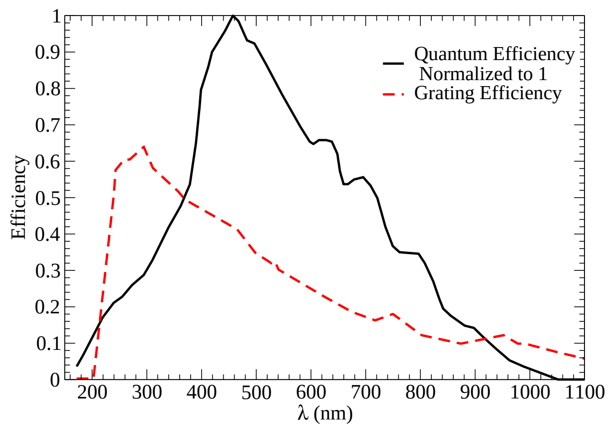

Figure 2: Quantum Efficiency of the AvaSpec-ULS2048L StarLine Versatile Fiber Optic Spectrometer's CCD is shown along with spectrometer's grating efficiency [31].

the only external components were a fiber to a spectrometer. The optics setup was sensitive in the 250–1100 nm range, limited by the transmission properties of the optical components used.

An AvaSpec-ULS2048L StarLine Versatile Fiber Optic Spectrometer [31], optimized for UV-light collection with a range of 200–1100 nm, was used to take the intensity vs wavelength data from the light emitted from the interactions between the alpha particles and the gas. This spectrometer is a charge coupled device (CCD) linear array with 2048 pixels, and the optical bench is a ULS Symmetrical Czerny-Turner with a 75 mm focal length. With a grating of 300 lines/mm and a slit size of 50 μm, the resolution of the spectrometer is 2.3 nm. The quantum efficiency for the CCD and the grating efficiency are shown in Figure 2.

For most configurations, 10 runs of 4-second integration times were taken to prevent saturation from a single long run. For runs with lower light emission, the integration time was increased. To align the optics, an LED light was placed at the focal point of the second parabolic mirror (see Figure 1). This created

0.22 NA fiber, and V2H6S 600 μm 0.22 NA feed-through were used.

a point at the object position of the setup. The optics stage with the mounted parabolic mirrors within the chamber was then adjusted to minimize the spot diameter from the LED. For this experiment, the object of the optical setup was taken to be the entry point of the beam in the chamber, found using film at the chamber beam entry port.

3. Transmission Measurements

To determine the transmission of the optical setup ideally, a light source transmitting through the entire range of the spectrometer would be used, and two spectra would be taken with this source: one with the mirrors, fibers, and feedthrough in place, and one without them (i.e. with the source shining directly into the spectrometer). However, a light source transmitting through the entire range of the spectrometer was unavailable. Instead, three light sources were used to obtain the transmission, each for a different range of wavelengths. A UV-Tool Shortwave Ultraviolet Flashlight was used to calculate transmission for the 250–380 nm range; a xenon arc lamp in a Solar Light Model XPS 400 power supply was used to calculate transmission in the 380–750 nm range; and the sun was used to calculate transmission in the 750–1100 nm range.

The UV flashlight had a fluorescent bulb producing well-defined peaks at 254, 314, 366, and 405 nm. Before the spectrum with the optics was compared to the spectrum without the optics, both spectra were normalized to the spectrometer's internal LEDs. The peaks obtained using the optics were divided by the peaks obtained without the optics in place to find transmission values for these points. A fit line was obtained for these individual points to interpolate transmission values for the wavelength range of 250–380 nm.

For the 380–750 nm range, a xenon arc lamp was used, but because of the arc lamp's high intensity, the beam of light was collimated with a pinhole. In order to stitch the 250–380 nm transmission spectrum from the UV flashlight to the 380–750 nm transmission spectrum from the xenon arc lamp, the transmission in the 330–380 nm range was averaged and ratioed for the two spectra. Multiplying the UV flashlight spectrum by this ratio, the transmission values in the UV flashlight spectrum were now relative to the transmission values in the xenon spectrum.

In the same way, the spectrum for the sun in the 750–1100 nm range was used for the transmission spectrum, with the 750–800 nm region being used to normalize the transmission values at the higher wavelengths from the sun to the midlength wavelengths from the xenon transmission measurement.

The entire transmission spectrum is shown in Figure 3.

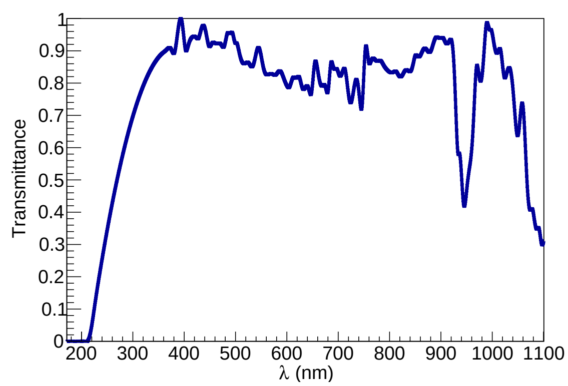

Figure 3: Relative transmission for the UV optical setup as a function of wavelength.

4. Analysis

There are eight internal LEDs in the spectrometer; these were enabled for the entire experiment and produce light at well-defined wavelengths of 211.7, 248.7, 365.5, 442.0, 612.6, 791.7, 936.6, and 1059.4 nm. Over the course of the experiment, these peaks did not shift, indicating that the spectrometer was very stable during the experiment to within the spectrometer digital resolution, corresponding to a bin width in the data of 0.6 nm. Because of this, runs with the same configuration (i.e. beam on/off and type of gas) were summed together successfully for better statistics.

LED calibration peaks were removed by subtracting the beam-off runs from the beam-on runs; this also accounted for background reduction from random noise and any other light sources. In some of the beam-off runs, the LED peaks were saturated. This was corrected for by scaling the saturated peaks before performing the subtraction (these scale factors were found by comparing saturated and unsaturated runs). Additionally, the beam-off and beam-on runs were scaled to unsaturated LED peaks before the subtraction occurred. After the background subtraction, shown in Figure 4 the data were scaled according to the relative optical transmission in Figure 3. Data were then normalized to the wavelength-dependent spectrometer sensitivity, provided by Avantes and shown in Figure 2.

5. Results

Spectra were found for alpha-induced luminescence in air, nitrogen, oxygen, and argon. The spectra for oxygen did not show any appreciable luminescence. We observed that while emission lines in N_2 were primarily in the 230–430 nm range, emission lines in air were mostly between 290–430 nm. Possible oxygen quenching in air is observed [32] as a deficiency of expected nitrogen lines in the 230–290 nm range. Several of the lines for the Ar spectra corresponding to emission lines found by Norlén (1973) have also been confirmed [33].

Spectra for N_2 are shown in Figure 4. This figure shows raw spectra, background spectra (beam off run), and the spectrum with the background subtracted.

Transmission-corrected spectra are shown in Figure 5 for Ar, O_2, and N_2, the latter both on- and off-axis. For the N_2 spectra, the intensity in the region below 290 nm differs between the on- and off-axis runs. It is thought that the increase in intensity is likely caused by molecular NO excitations (Gamma bands from 200-270 nm and Delta bands from 200-240 nm [34], noted in Figure 5b) as the beam enters the plastic window of the detector, though this has yet to be confirmed with certainty. The reasoning is that the presumed NO lines in the off-axis runs have a higher relative intensity than for the on-axis runs. The

(a) Beam-on run

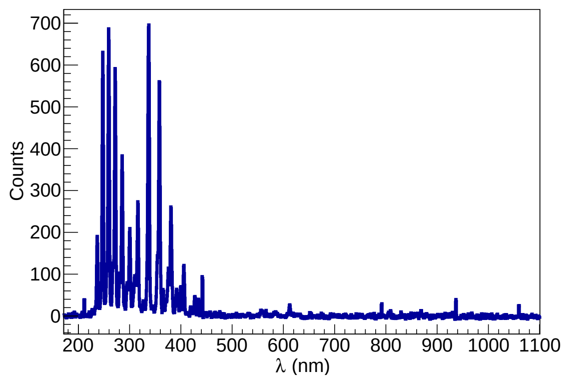

(b) Beam-off run

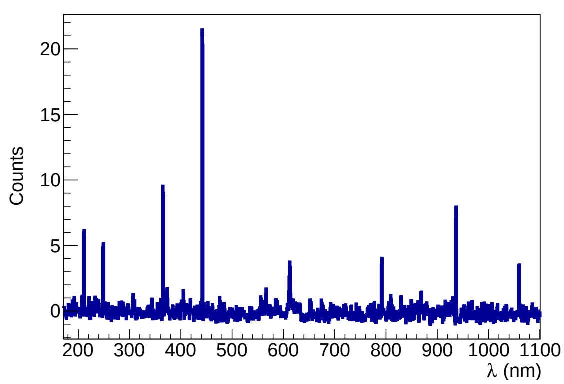

(c) Subtracted beam-off from beam-on

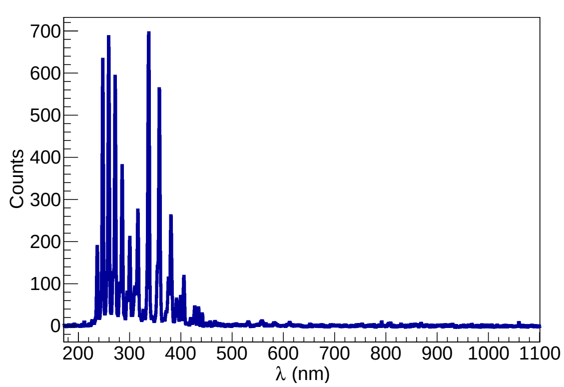

Figure 4: N_2 raw spectra (a) shown for a 140-second run. The background spectrum from a 40-second run is scaled (b) before subtraction (c).

optical setup in the off-axis runs are focused on the beam entry point in the chamber. At this point, only photons produced at the chamber entry are focused into the optical setup. However, for the beam on-axis runs, all photons traveling parallel to the beam direction, including those produced at the Bragg peak, are focused into the optical setup. It is expected that the presumed NO lines are from the chamber window and light producing these lines are produced in or near the chamber window. Thus, when the optics are focused on the chamber window, a larger proportion of light from NO is expected, whereas, when the optics are on-axis, a larger proportion of light produced at the Bragg peak is expected.

Transmission-corrected spectra for air are shown in Figure 6. The UV-vis region of 300–400 nm shows the results of this work as well as detector-uncorrected data from alpha-induced luminescence [7] and electron-induced luminescence [3].

6. Conclusions

Alpha-induced luminescence measurements of nitrogen, oxygen, argon, and air emission lines from 5 MeV alpha particles were made. For air, N_2, and Ar, we found 12, 16, and 18 dominant lines respectively in the spectral ranges 270–430 nm, 230–430 nm, and 690–970 nm. Spectra were background-subtracted and corrected for transmission and detector efficiency. Evidence of oxygen-quenching was found, and it was determined that argon had little effect on the luminescence in air, but a strong signature in the near infrared region, as expected [8, 35]. Measurements of alpha-induced luminescence could reduce background while maximizing signal by using a narrow band filter corresponding to the strongest emission peaks for each gas.

For air, the spectral range was extended below that of previous electron-induced luminescent spectra [3] to the deep UV range. Because natural background in the deep UV is low, detectors may be optimized to collect this signal. Additionally, these spectra show that in situations where feasible using a nitrogen purge gas would greatly reduce the effect of oxygen quenching the NO lines,

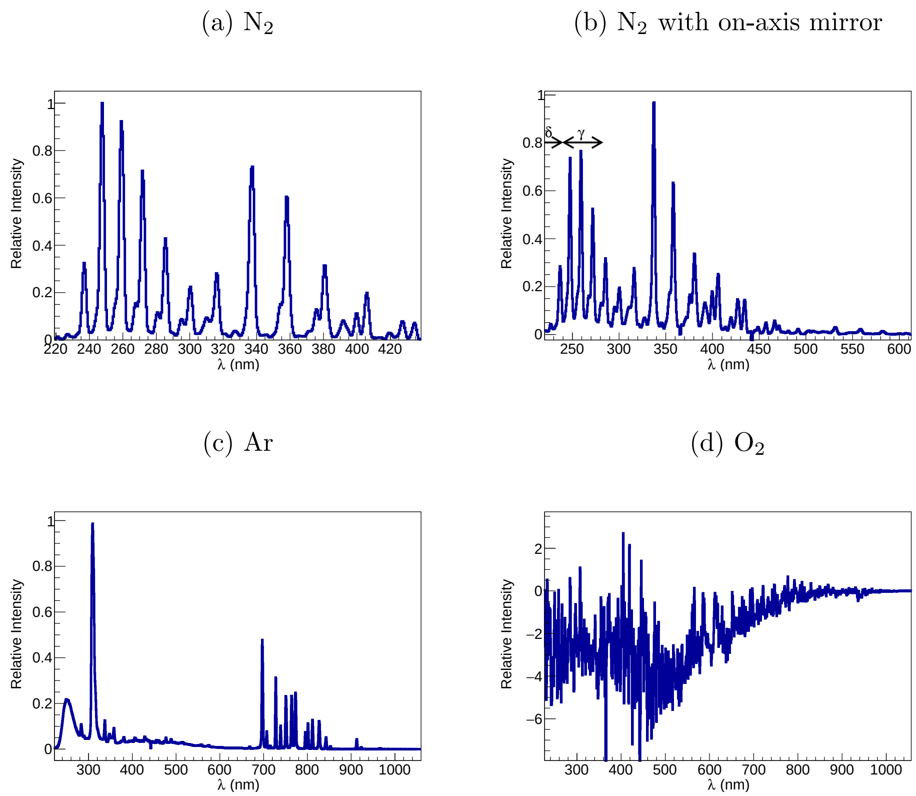

Figure 5: Transmission-corrected alpha-induced luminescence spectra for N_2, Ar, and O_2. N_2 spectra are normalized to the 337 nm peak and the delta and gamma bands are noted Figure 5(b). The Ar spectrum is normalized to the tallest peak at 312 nm. The O_2 spectrum shows no useable lines for measuring alpha-induced luminescence.

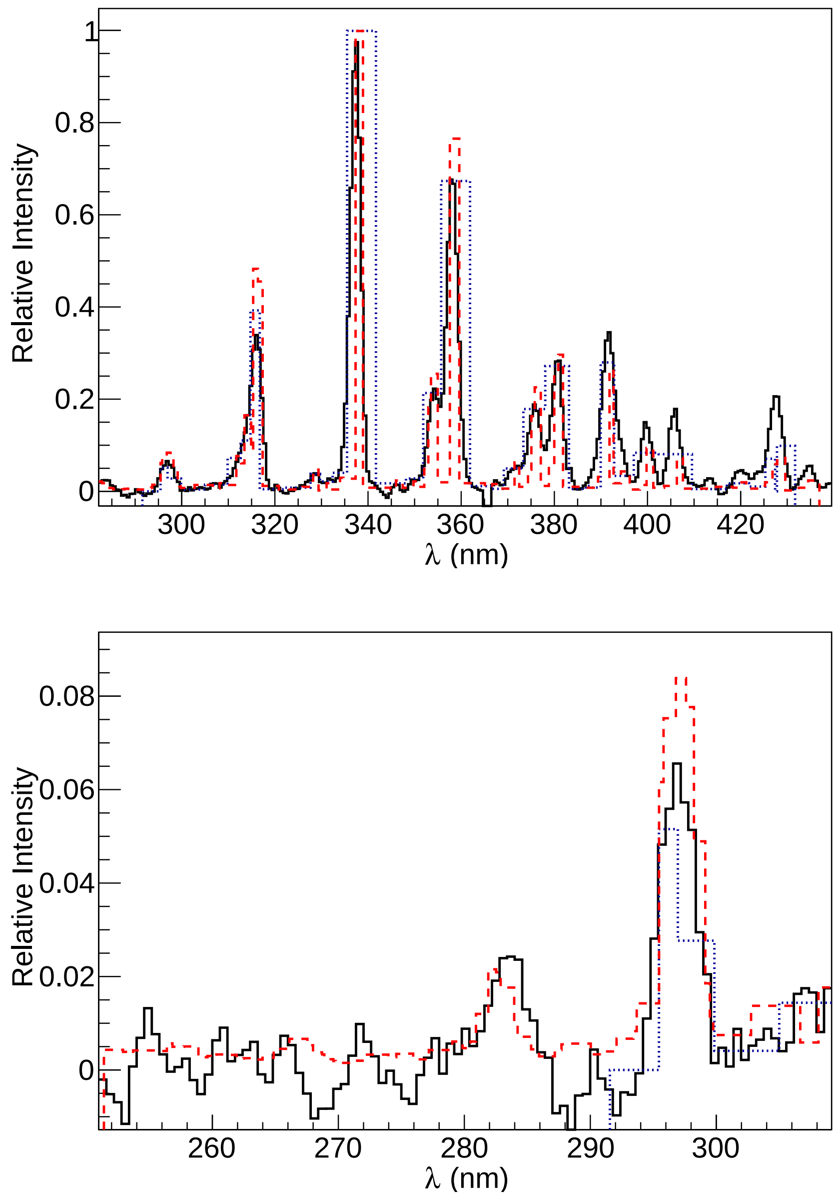

Figure 6: Transmission-corrected alpha-induced luminescence spectra for air in the UV-VIS region (top) and deep UV (bottom). This work is shown in solid black, alpha-induced luminescent data from [7] are shown in dashed red, and electron-induced luminescent data from [3] are shown in dotted blue. All spectra are normalized to the N_2 337 nm peak.

raising signal intensity without affecting the light background.

To date there have been few experiments with filters to maximize light collection, while minimizing background. Baschenko [5] used an optical glass filter with 60% transparency in the 300–400 nm range to maximize signal collection, Inrig, et al. [15] used a customized UG-11 filter, and Sand, et al. [7, 21, 22] found stacks of various Semrock single interference filters could be used to improve the signal-to-background ratio. Lakis, et al. studied various filters, including combinations of Semrock filters with KG1 colored glass [24]. Chroma filters and a Channel Systems custom filter both offer decent transmission with good visible light blocking. Transmission of leaded glass and plexiglass were also studied. The current state is a call for custom filters to reduce transmission in the visible light spectrum and increase transmission in the alpha-induced luminescence region. No studies have been done yet to optimize filters for pure gas environments like N_2 and Ar. Spectra from this work can be used to optimize filters or determine operating parameters.

In addition to effects from filtering, future work may focus on the pressure dependence for alpha-induced luminescence yields or for other gases. In particular, photon intensity depends on the gas and composition, with some gases having an increased yield [36]. This presents the possibility of optimizing the detector-gas system for specific applications. This would include exploring yields for various particles at various energies and for various wavelengths.

Acknowledgements

This work was sponsored by the U.S. Department of Energy (DOE), National Nuclear Security Administration (NNSA), Office of International Nuclear Safeguards (NA-241), Safeguards Technology Development Program. We would like to acknowledge Andrew Famiano, for his help in aligning the optics.

References

[1] M. Fraga, A. Onofre, L. Pereira, N. Castro, F. Veloso, F. Fraga, R. F. Marques, M. Pimenta, A. Policarpo, Temperature-dependent quenching of uv fluorescence of n 2, Nuclear Instruments and Methods in Physics Research Section A: Accelerators, Spectrometers, Detectors and Associated Equipment 597 (1) (2008) 75–82.

[2] R. Abbasi, T. Abu-Zayyad, K. Belov, J. Belz, Z. Cao, M. Dalton, Y. Fedorova, P. Hüntemeyer, B. Jones, C. Jui, E. Loh, N. Manago, K. Martens, J. Matthews, M. Maestas, D. Rodriguez, J. Smith, P. Sokolsky, R. Springer, J. Thomas, S. Thomas, P. Chen, C. Field, C. Hast, R. Iverson, J. Ng, A. Odian, K. Reil, D. Walz, D. Bergman, G. Thomson, A. Zech, F.-Y. Chang, C.-C. Chen, C.-W. Chen, M. Huang, W.-Y. Hwang, G.-L. Lin, Air fluorescence measurements in the spectral range 300-420nm using a 28.5GeV electron beam, Astropart. Phys. 29 (1) (2008) 77–86. `doi:10.1016/j.astropartphys.2007.11.010`.
URL `http://www.sciencedirect.com/science/article/pii/S0927650507001715`

[3] M. Ave, M. Bohacova, B. Buonomo, N. Busca, L. Cazon, S. Chemerisov, M. Conde, R. Crowell, P. Di Carlo, C. Di Giulio, M. Doubrava, A. Esposito, P. Facal, F. Franchini, J. Hrandel, M. Hrabovsky, M. Iarlori, T. Kasprzyk, B. Keilhauer, H. Klages, M. Kleifges, S. Kuhlmann, G. Mazzitelli, L. Nozka, A. Obermeier, M. Palatka, S. Petrera, P. Privitera, J. Ridky, V. Rizi, G. Rodriguez, F. Salamida, P. Schovanek, H. Spinka, E. Strazzeri, A. Ulrich, Z. Yusof, V. Vacek, P. Valente, V. Verzi, T. Waldenmaier, Measurement of the pressure dependence of air fluorescence emission induced by electrons, Astroparticle Physics 28 (2007) 41–57.

[4] T. Waldenmaier, H. Blumer, Spectral resolved measurement of the nitrogen fluorescence yield in air induced by electrons, Astroparticle Physics 29 (2008) 205.

[5] S. M. Baschenko, Remote optical detection of alpha particle sources, J. Radiol. Prot. 24 (1) (2004) 75–82. doi:10.1088/0952-4746/24/1/006. URL http://iopscience.iop.org/article/10.1088/0952-4746/24/1/006http://stacks.iop.org/0952-4746/24/i=1/a=006?key=crossref.ffe22bb4f3a1e2d49f5da2625baed691

[6] J. Sand, S. Ihantola, K. Peräjärvi, H. Toivonen, J. Toivonen, Radioluminescence yield of alpha particles in air, New J. Phys. 16 (5) (2014) 053022. doi:10.1088/1367-2630/16/5/053022. URL http://stacks.iop.org/1367-2630/16/i=5/a=053022?key=crossref.f054b937ee8bf3c9e030af451ca3179b

[7] J. Sand, Alpha Radiation Detection via Radioluminescence of Air, Tampere University of Technology Thesis., Tampere University of Technology, 2016. URL https://tutcris.tut.fi/portal/files/9072621/sand_1449.pdf

[8] S. Dondes, P. Harteck, C. Kunz, A spectroscopic study of alpha-ray-induced luminescence in gases: Part i, Radiation Research 27 (2) (1966) 174–210. URL http://www.jstor.org/stable/3571909

[9] P. P. Bachelor, D. V. Jordan, W. W. Harper, B. D. Cannon, E. C. Finn, Self-absorption effects on alpha-induced atmospheric nitrogen fluorescence yield, J. Radioanal. Nucl. Chem. 282 (3) (2009) 873–876. doi:10.1007/s10967-009-0331-0. URL http://link.springer.com/10.1007/s10967-009-0331-0

[10] F. Lamadie, F. Delmas, C. Mahe, P. Girones, C. Le Goaller, J. Costes, Remote alpha imaging in nuclear installations: new results and prospects, IEEE Trans. Nucl. Sci. 52 (6) (2005) 3035–3039. doi:10.1109/TNS.2005.862911. URL http://ieeexplore.ieee.org/lpdocs/epic03/wrapper.htm?arnumber=1589317http://ieeexplore.ieee.org/document/1589317/

[11] T. Cousins, D. S. Haslip, Stand and Deliver, CBRNe World Winter (2006) 56–59.

URL http://www.cbrneworld.com/{_}uploads/download{_}magazines/STAND{_}AND{_}DELIVER.pdf

[12] D. Chichester, S. Pozzi, E. Seabury, J. Dolan, M. Flaska, J. Johnson, S. Watson, J. Wharton, Fy09 advanced instrumentation and active interrogation research for safeguards, Idaho National Laboratory, Idaho Falls, ID, INL/EXT-09-16611, (2010).

[13] D. L. Chichester, S. M. Watson, Multispectral UV-visual imaging as a tool for locating and assessing ionizing radiation in air, in: IEEE Nucl. Sci. Symp. Med. Imaging Conf., IEEE, 2010, pp. 447–453. doi:10.1109/NSSMIC.2010.5873799.
URL http://ieeexplore.ieee.org/document/5873799/

[14] E. Inrig, L. Erhardt, V. Koslowsky, B. Andrews, H. Ing, M. Dick, P. Forget, An air fluorescence imaging system for the detection of radiological contamination, Vol. 8018, 2011, p. 80180G. doi:10.1117/12.887352.
URL http://proceedings.spiedigitallibrary.org/proceeding.aspx?doi=10.1117/12.887352

[15] E. Inrig, V. Koslowsky, B. Andrews, M. Dick, P. Forget, H. Ing, R. Hugron, L. Wong, M. E. Hamm, R. W. Hamm, Development and Testing of an Air Fluorescence Imaging System for the Detection of Radiological Contamination, in: AIP Conf. Proc. 1412, Vol. 393, AIP Publishing, 2011, pp. 393–400. doi:10.1063/1.3665340.
URL http://link.aip.org/link/APCPCS/v1412/i1/p393/s1{&}Agg=doihttp://scitation.aip.org/content/aip/proceeding/aipcp/10.1063/1.3665340http://aip.scitation.org/doi/abs/10.1063/1.3665340

[16] O. P. Ivanov, V. E. Stepanov, S. V. Smirnov, A. G. Volkovich, Development of method for detection of alpha contamination with using UV-camera DayCor by OFIL, in: 2011 IEEE Nucl. Sci. Symp. Conf. Rec., IEEE, 2011, pp.

2192–2194. doi:10.1109/NSSMIC.2011.6154448.
URL http://ieeexplore.ieee.org/document/6154448/

[17] J. Yao, J. Brenizer, R. Hui, S. Yin, Standoff alpha radiation detection via excited state absorption of air Development and irradiation test of lost alpha detection system for Collisional-radiative model in air for earth re-entry problems Standoff alpha radiation detection via excited state , Cit. Appl. Phys. Lett. J. Appl. Phys.4930888 Rev. Sci. Instrum. ITERa) Rev. Sci. Instrum. Phys. Plasmas 102 (13) (2013) 254101–114502. doi:10.1063/1.2194827.
URL http://dx.doi.org/10.1063/1.4812338http://scitation.aip.org/content/aip/journal/apl/102/25?ver=pdfcov

[18] J. S. Feener, W. S. Charlton, Preliminary results of nuclear fluorescence imaging of alpha and beta emitting sources, in: 2013 3rd International Conference on Advancements in Nuclear Instrumentation, Measurement Methods and their Applications (ANIMMA), 2013, pp. 1–8. doi:10.1109/ANIMMA.2013.6728086.

[19] N. Kume, K. Takakura, K. Nakayama, H. Kuroda, M. Izumi, N. Mukai, Remote detector of alpha-ray using ultraviolet ray emitted by nitrogen in air, in: 2013 IEEE Nucl. Sci. Symp. Med. Imaging Conf. (2013 NSS/MIC), IEEE, 2013, pp. 1–6. doi:10.1109/NSSMIC.2013.6829621.
URL http://ieeexplore.ieee.org/document/6829621/

[20] J. Sand, V. Hannuksela, J. Toivonen, S. Ihantola, K. Peraejaervi, H. Toivonen, Remote optical detection of alpha radiation, (IAEA-CN–184), (2010).

[21] J. Sand, S. Ihantola, K. Peräjärvi, A. Nicholl, E. Hrnecek, H. Toivonen, J. Toivonen, Imaging of alpha emitters in a field environment, Nucl. Inst. Meth. A 782 (2015) 13–19. doi:10.1016/j.nima.2015.01.087.
URL https://www.researchgate.net/publication/272395964{_}Imaging{_}of{_}Alpha{_}Emitters{_}in{_}a{_}Field{_}Environment

[22] J. Sand, A. Nicholl, E. Hrnecek, H. Toivonen, J. Toivonen, K. Perajarvi, Stand-Off Radioluminescence Mapping of Alpha Emitters Under Bright Lighting, IEEE Trans. Nucl. Sci. 63 (3) (2016) 1777–1783. doi:10.1109/TNS.2016.2562359.
URL http://ieeexplore.ieee.org/document/7465773/

[23] J. Sand, S. Ihantola, K. Peräjärvi, H. Toivonen, J. Toivonen, Optical detection of radon decay in air, Sci. Rep. 6 (1) (2016) 21532. doi:10.1038/srep21532.
URL http://www.nature.com/articles/srep21532

[24] R. E. Lakis, K. E. Koehler, V. Henzl, A. Pugmire, A. Favalli, D. Desimone, M. Browne, Imaging alpha-induced radioluminescence using the digital cherenkov viewing device, Proc. of the 56th INMM Annual Meeting.

[25] G. ORTNER, S. SALIM, Light Emission from Polonium, Nature 169 (4312) (1952) 1060–1061. doi:10.1038/1691060b0.
URL http://www.nature.com/doifinder/10.1038/1691060b0

[26] R. W. NICHOLLS, E. M. REEVES, Luminescence produced in Air by Polonium-210 α-Particles, Nature 180 (4596) (1957) 1188–1189. doi:10.1038/1801188a0.
URL http://www.nature.com/doifinder/10.1038/1801188a0

[27] W. Huggins, L. Huggins, On the Spectrum of the Spontaneous Luminous Radiation of Radium. Part III. Radiation in Hydrogen, Proc. Phys. Soc. 76 (512) (1905) 488–492.
URL http://dx.doi.org/10.1098/rspa.1905.0054

[28] T. D. Strickler, E. T. Arakawa, Optical Emission from Argon Excited by Alpha Particles: Quenching Studies, J. Chem. Phys. 41 (6) (1964) 1783–1789. doi:10.1063/1.1726158.
URL http://aip.scitation.org/doi/10.1063/1.1726158

[29] J. B. Birks, The Theory and Practice of Scintillation Counting: International Series of Monographs in Electronics and Instrumentation, Vol. 27, Elsevier, 2013.

[30] J. F. Ziegler, Srim-2003, Nuclear instruments and methods in physics research section B: Beam interactions with materials and atoms 219 (2004) 1027–1036.

[31] Avantes, AvaSpec-ULS2048 StarLine Versatile Fiber-optic Spectrometer - Avantes.
URL `https://www.avantes.com/products/spectrometers/starline/item/208-avaspec-uls2048-starline-versatile-fiber-optic-spectrometer`

[32] G. M. Barenboim, Quenching of photoluminescence of biomolecules by oxygen and nitric oxide, Biofizika 8 (1963) 321.

[33] G. Norlén, Wavelengths and energy levels of ar i and ar ii based on new interferometric measurements in the region 3 400-9 800 å, Physica Scripta 8 (6) (1973) 249.

[34] R. Huffman, F. LeBlanc, J. Larrabee, D. Paulsen, Satellite vacuum ultraviolet airglow and auroral observations, Journal of Geophysical Research: Space Physics 85 (A5) (1980) 2201–2215. `doi:10.1029/JA085iA05p02201`.
URL `http://dx.doi.org/10.1029/JA085iA05p02201`

[35] A. Kramida, Yu. Ralchenko, J. Reader, and NIST ASD Team, NIST Atomic Spectra Database (ver. 5.3), [Online]. Available: `http://physics.nist.gov/asd` [2017, August 21]. National Institute of Standards and Technology, Gaithersburg, MD. (2015).

[36] C. E. Melton, G. S. Hurst, T. E. Bortner, Ionization produced by 5-mev alpha particles in argon mixtures, Phys. Rev. 96 (1954) 643–645. `doi:10.1103/PhysRev.96.643`.
URL `https://link.aps.org/doi/10.1103/PhysRev.96.643`